Statistical Models for Temperature Prediction in Civil Structures

CHIARA SUPPI, CLAUDIA GIRARDI, ALESSANDRO LOTTI, DANIELE ZONTA and ALESSANDRO PRADA

ABSTRACT

This paper presents two models for reconstructing the thermal field of civil structures without relying on thermocouple data, using instead information from weather stations located near the structure under analysis. The first model estimates temperature through a linear correlation with air temperature, while the second adopts a physics-based approach that also accounts for the effects of solar radiation. Both models were applied to the bell tower of Portogruaro. The physics-based model demonstrated high accuracy, with a prediction uncertainty of 1.50 °C and a correlation coefficient of 0.99 between predicted and measured temperatures.

INTRODUCTION

Structural health monitoring plays a crucial role in ensuring the safety, operational efficiency, and long-term durability of civil infrastructure. Among the various factors influencing structural behavior, temperature is generally the dominant one. Both daily and seasonal thermal fluctuations induce deformations that can substantially distort monitoring data, potentially compromising the interpretation of the structural mechanical response [1] [2]. Therefore, accurate temperature compensation is essential to isolate thermal effects from actual structural deformations. Such compensation requires a comprehensive characterization of the thermal field acting on the structure. The temperature distribution within a structure is influenced by numerous factors, including material properties, solar radiation, ventilation conditions, and geometry. As a result, the thermal field is complex and varies spatially and temporally, making its evolution difficult to predict without direct measurements.

Chiara Suppi, Department of Civil Engineering, University of Trento, Trento, Italy

Currently, the most widespread technology for direct temperature monitoring involves using thermocouples, which are typically installed permanently for the entire monitoring duration [3] [4]. Despite their utility, these sensors are prone to faults and failures over time, often leading to data gaps or the collection of unreliable information.

These limitations highlight the need for alternative approaches capable of estimating the thermal field of a structure even without direct temperature measurements. Previous studies have proposed the use of data from nearby meteorological stations to estimate the thermal behavior of structures [5] [6]. The simplest approach is to consider the structural temperature as spatially uniform and equal to the ambient air temperature. While this may provide acceptable results for seasonal compensation, it fails to account for daily thermal variations, which are largely governed by temperature gradients within the same structural element.

In general, predicting the thermal field of a structure *a priori* with sufficient accuracy remains challenging, even with the support of meteorological data. Nevertheless, this study demonstrates that accurate thermal prediction becomes feasible after a limited observational period. It is shown that, following a brief calibration phase, it is possible to develop a statistical model that reliably estimates the temperature profile using data from meteorological stations.

Two statistical models are investigated:

- **Model A** assumes a correlation between air temperature and the thermal field of the structure, assuming synchronous variations.
- **Model B** introduces the concept of structural thermal inertia, computing temperature through a simplified thermodynamic energy balance driven by air temperature and solar radiation.

The proposed models have been validated on the bell tower of Portogruaro (Venice, Italy), a monitored heritage structure that experienced numerously discontinuities in its temperature sensing system.

The paper is organized as follows: Section 2 introduces the developed models; Section 3 presents the case study; Section 4 reports and discusses the results; and Section 5 outlines the main conclusions and future research directions.

FORMULATION

This chapter presents two models developed to estimate the thermal field of a structure using limited information provided by a nearby meteorological station.

Model A

Model A is a synchronous linear model that establishes a direct relationship between the temperature measured by a thermocouple installed within the structure and the atmospheric temperature recorded by a nearby weather station. The model is expressed by the following equation:

$$T_{j,i} = q_j + m_j \cdot T_{0,i} \tag{1}$$

where $T_{j,i}$ represents the temperature recorded by the thermocouple j at time i, and T_0 is atmospheric temperature measured by the weather station at the same time.

The model was calibrated using the least squares method to estimate the parameters q and m.

Model B

Unlike Model A, Model B accounts for the thermal inertia of the structure and the resulting time-dependent behavior of temperature. It is based on the energy balance of thermal systems with lumped capacity, following the Lumped Capacitance Method, which assumes no internal temperature gradients within the analyzed element [7] [8]. The governing energy equation is expressed as:

$$\frac{dE}{dt} = C \cdot \frac{dT}{dt} \tag{2}$$

where E denotes the thermal energy stored in the system (J), and C is the total thermal capacity (J/°C), which depends on the material and the size of the considered element.

Equation (2), applied to a structure, can be made explicit by including all the main energy contributions involved, such as the power absorbed from solar radiation ($\dot{Q}_{sol.}$), the power generated by internal heat sources ($\dot{Q}_{int.}$), thermal losses due to conduction and convection through the building surfaces ($\dot{Q}_{disp.}$), and heat exchanges caused by ventilation ($\dot{Q}_{vent.}$).

The Model B developed in this study considers only the energy contributions associated with solar radiation and thermal losses, neglecting the effects of internal heat sources and ventilation. As a result, Equation (2) can be rewritten as follows:

$$\dot{Q}_{sol.} - \dot{Q}_{disp.} = C \cdot \frac{dT}{dt} \tag{3}$$

The solar power is determined by:

$$\dot{Q}_{sol.} = \alpha \cdot G \cdot A_{irr} \tag{4}$$

where α is the absorption coefficient, which depends on the material's properties, G is the incident solar radiation intensity (W/m²) and A_{irr} is the exposed surface area (m²).

The dissipated power, on the other hand, depends on:

$$Q_{disp.} = \left(h + \frac{\lambda}{s}\right) \cdot A_{disp} \cdot (T_{in} - T_{out}) \tag{5}$$

In Equation (5), h represents the convective heat transfer coefficient (W/m²·K), which quantifies the heat exchange between the surface and the surrounding air through convection; its value depends on the properties of the fluid, the flow conditions, and the geometry of the surface. The parameter λ is the thermal conductivity of the material (W/m·K), indicating its ability to conduct heat, while s

is the thickness of the material (m). The ratio λ/s therefore represents the conductive thermal transmittance through the material layer. A_{disp} denotes the heat-dissipating surface area (m²), and T_{in} and T_{out} correspond to the internal and external (air) temperatures, respectively.

By grouping the terms using the coefficients $\hat{\alpha} = \alpha \cdot A_{irr}$, defined as the equivalent irradiated area, and $\sigma = (h + \lambda/s) \cdot A_{disp}$, representing a global dispersion coefficient for conduction and convection, and denoting $T_{j,i}$ the temperature recorded by the thermocouple j at the time i, and with $T_{0,i}$ the air temperature recorded by the weather station at the same time, the energy balance can be reformulated as follows:

$$\hat{\alpha} \cdot G_i - \sigma \cdot (T_{j,i} - T_{0,i}) = C \cdot \frac{dT_{j,i}}{dt} \tag{6}$$

The temperature is then computed using the finite difference method, which allows the estimation of the temperature at the next time step T_{i+1} through the following expression:

$$\frac{\hat{\alpha}}{C} \cdot G_i - \frac{\sigma}{C} \cdot \left(T_{j,i} - T_{0,i}\right) = \frac{T_{j,i+1} - T_{j,i}}{\Delta t} \tag{7}$$

The model was calibrated using the least squares method to estimate the parameters $\theta_1 = \hat{\alpha}/C$ and $\theta_2 = \sigma/C$.

CASE STUDY

The bell tower of the Cathedral of Sant'Andrea in Portogruaro (VE) (Figure 1a) is a 59 m masonry structure. The tower has a square footprint, with side lengths tapering from 7.30 meters at the base to 6.45 meters at the top. Wall thickness decreases from 1.3 meters at the base to 0.9 meters at the top. Inside, the tower contains four wooden floors and two masonry cross vaults. The upper section houses the bell chamber, which is topped by an octagonal drum and a 15.84 m pyramidal spire. The tower leans toward the northeast, with a tilt that varies along its height, as shown in Figure 1b.

A continuous monitoring system has been in operation since 2003. Its primary instrument is a 29.90 m pendulum with a brass mass submerged in water to dampen oscillations. The pendulum's position is recorded every 10 minutes using two digital cameras. The system also includes four type-K thermocouples (T1-T4): two placed on the exterior (T1 and T3) and two embedded in the masonry (T2 and T4), all recording temperature every 10 minutes. Additional components include a robotic total station, SOFO fiber optic sensors, load cells, and crack meters [9].

The thermocouples have proven to be the most problematic part of the system due to frequent data interruptions. These gaps required reconstructing the thermal field using the predictive models (Model A and Model B) described in the previous section. Both models use data from the Portogruaro-Lison weather station, located 7 km from the bell tower.

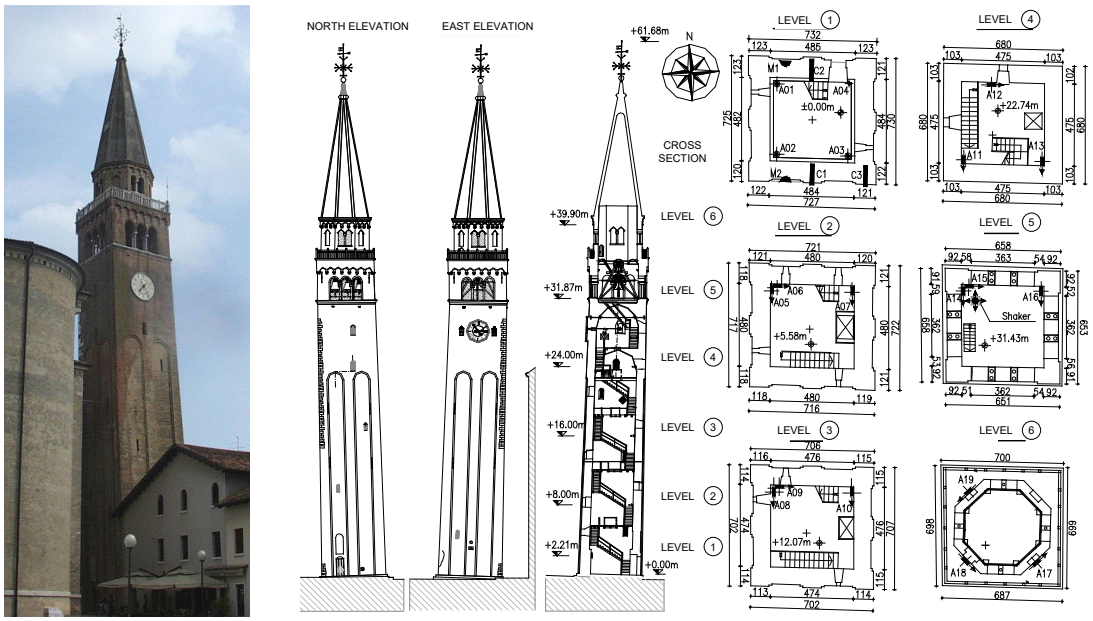

a) b)

Figure 1. a) Bell tower of the Cathedral of Sant'Andrea (Portogruaro, VE); b) North and East elevation, cross-section and plan views at different levels

RESULTS

The results are presented starting with the calibration of the model parameters, followed by the temperature prediction phase. The model's accuracy is assessed using two main metrics: the standard deviation σ_j, which quantifies the average prediction error, and the coefficient of determination R_j^2, which indicates how well the predicted values $\hat{T}_{j,i}$ align with the measured temperatures $T_{j,i}$.

$$\sigma_j = \sqrt{\frac{1}{n-1}\sum_{i=1}^{n}\left(T_{j,i} - \hat{T}_{j,i}\right)^2} \tag{8}$$

$$R_j^2 = 1 - \frac{\sum_{i=1}^{n}\left(T_{j,i} - \hat{T}_{j,i}\right)^2}{\sum_{i=1}^{n}\left(T_{j,i} - \mu_{T_j}\right)^2} \tag{9}$$

Model A

Model A was calibrated on two datasets. The complete temperature dataset, with measurements recorded every 10 minutes which provided the parameters q_{10min} and m_{10min}. A reduced dataset based on a single daily measurement taken at 5:00 AM which provided the parameters q_{5AM} and m_{5AM}. Table I reports the calibrated q and m parameters for each thermocouple.

TABLE I. Parameter calibration results for Model A

Thermocouple	q_{10min}	m_{10min}	q_{5AM}	m_{5AM}
T1	3.96	0.94	5.05	1.10
T2	4.80	0.82	5.74	1.00
T3	4.49	0.95	5.63	1.11
T4	4.72	0.83	5.58	1.00

Once the model parameters were calibrated, three prediction scenarios were implemented. The first scenario, ModelA_1, uses 10-minute interval data both for calibration and prediction. The second, ModelA_2, is specifically designed for temperature values recorded at 5:00 AM. In this case, the model is calibrated and applied solely on that subset. Finally, the third scenario, ModelA_3, uses parameters calibrated on 5:00 AM data to predict the full time series with 10-minute resolution. Table II reports the results obtained for each model, expressed through the accuracy metrics defined in Equations (8) and (9).

TABLE II. Temperature prediction results using Model A

Thermocouple	ModelA_1		ModelA_2		ModelA_3	
	σ	R^2	σ	R^2	σ	R^2
T1	3.91 °C	0.81	2.81 °C	0.89	4.14 °C	0.65
T2	3.74 °C	0.78	2.83 °C	0.87	4.04 °C	0.56
T3	3.97 °C	0.81	3.02 °C	0.88	4.19 °C	0.66
T4	3.67 °C	0.78	2.67 °C	0.88	3.96 °C	0.58

Model B

Table III summarizes the calibrated parameters θ_1 and θ_2 of Model B for each thermocouple, obtained using the full dataset with 10-minute interval measurements. The table also reports the model's accuracy in predicting temperatures, evaluated using the metrics defined in Equations (8) and (9).

TABLE III. Parameter calibration and temperature prediction results for Model B

Thermocouple	Parameter calibration		Temperature prediction	
	θ_1	θ_2	σ	R^2
T1	$1.29 \cdot 10^7$	$6.13 \cdot 10^7$	1.32 °C	0.98
T2	$1.95 \cdot 10^8$	$1.97 \cdot 10^8$	0.93 °C	0.97
T3	$1.38 \cdot 10^7$	$5.82 \cdot 10^7$	1.49 °C	0.97
T4	$2.82 \cdot 10^8$	$3.24 \cdot 10^8$	1.19 °C	0.96

Discussion

Figure 2 presents the results obtained for thermocouple T1 using models A_1, A_2, A_3, and B. The black line represents the temperature measured by the thermocouple, while the blue line shows the corresponding model predictions. For each model, the comparison is illustrated on three levels:

(a) annual trend for the year 2011,
(b) detailed view over a 5-day period (April 15-20, 2011),
(c) correlation between predicted and measured temperatures, evaluated using the Pearson correlation coefficient.

The red box in plots (a) highlights the time interval shown in detail in the corresponding plots (b).

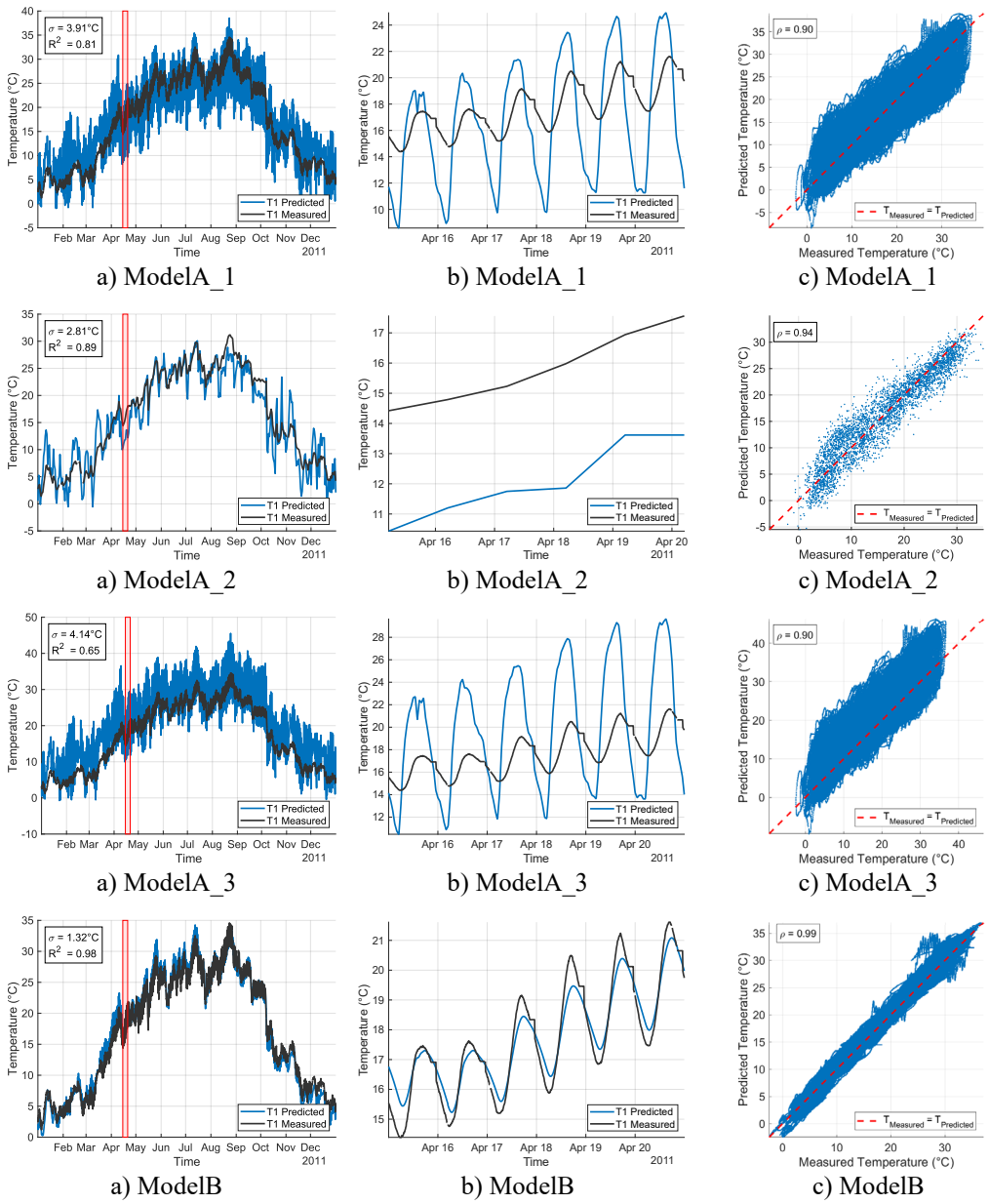

Figure 2. Results related to thermocouple T1 using the predictive model A and B: a) 1 year time series; b) 5 days zoom; c) correlation between predicted and measured temperatures

The results show improved predictive performance from ModelA_1 ($\sigma = 3.91$ °C) to ModelA_2 ($\sigma = 2.81$ °C), due to using 5:00 AM data, when temperatures are more stable and less affected by solar input. However, both are in-sample models, meaning calibration and prediction rely on the same dataset. ModelA_3, using 5:00 AM parameters to predict 10min-resolution data, performs worse ($\sigma \approx 4$ °C), which is too high for reliable use. All Model A setups show a time lag caused by thermal inertia. Model B, which includes physical heat transfer processes, performs better ($\sigma <$ 1.50 °C). This uncertainty falls within the thermocouple accuracy range (0.5-1.0 °C), confirming its reliability. The correlation plot for Model B (c) shows a Pearson coefficient of $\rho = 0.99$, with predicted and observed temperatures tightly aligned along the bisector.

CONCLUSIONS

This study developed a predictive model for assessing the thermal behavior of civil structures, using the bell tower of Portogruaro as a case study. The methodology involved the stepwise development of two models with increasing complexity: an initial synchronous linear model based solely on air temperature data from a weather station (Model A), followed by an enhanced formulation that also accounts for solar radiation (Model B).

Results demonstrate substantial gains in predictive accuracy. Model B reduces the standard deviation from approximately 4°C to 1.50°C, which is consistent with the operational precision of thermocouple sensors. Simultaneously, the coefficient of determination improves from 0.60 to near-unity values, indicating excellent agreement between predicted and measured temperatures. These outcomes position Model B as a promising tool for future research, including its application to other civil structures and the exploration of strategies to define the minimum optimal period for sensor installation. Such an approach would enable sensor removal after a limited monitoring phase while maintaining accurate thermal predictions through the model, substantially reducing the long-term costs of thermal monitoring systems.

ACKNOWLEDGEMENTS

This study was supported and funded by the ReLUIS Interuniversity Consortium and the European Union-Next Generation EU program (Mission 4, Component 2; CUP: E53D23003560006). The authors also wish to express their sincere gratitude to the Municipality of Portogruaro for granting access to the monitoring data of the bell tower and thank the technical staff for their support in the maintenance and operation of the monitoring system.

REFERENCES

[1] Han, Q., Q. Ma, J. Xu, and M. Liu. February 2021. “Structural Health Monitoring Research under Varying Temperature Condition: A Review,” *J. Civil Struct. Health Monit.*, 11(1):149-173.

[2] Peeters, B. and G. De Roeck. 2001. “One-Year Monitoring of the Z24-Bridge: Environmental Effects versus Damage Events,” *Earthq. Eng. Struct. Dyn.*, 30(2):149-171.

[3] Bajzek, T. J. March 2005. “Thermocouples: A Sensor for Measuring Temperature,” *IEEE Instrum. Meas. Mag.*, 8(1):35-40.

[4] Pollock, D. D. 1971. *The Theory and Properties of Thermocouple Elements*. Philadelphia: American Society for Testing & Materials, in ASTM Special Technical Publication.

[5] Zhang, Q., G. Dai, and Y. Tang. January 2022. “Thermal Analysis and Prediction Methods for Temperature Distribution of Slab Track Using Meteorological Data,” *Sensors*, 22(17):6345.

[6] Westphal, F. S. and R. Lamberts. August 2004. “The Use of Simplified Weather Data to Estimate Thermal Loads of Non-Residential Buildings,” *Energy Build.*, 36(8):847-854.

[7] Bejan, A. March 2022. *Heat Transfer: Evolution, Design and Performance*. Hoboken: John Wiley & Sons.

[8] Arregi, B., R. Garay-Martinez, and J. C. Ramos. October 2023. “Estimation of Thermal Resistance and Capacitance of a Concrete Wall from In Situ Measurements: A Comparison of Steady-State and Dynamic Models,” *Energy Build.*, 296:113393.

[9] Zonta, D. and M. Pozzi. December 2015. “The Remarkable Story of Portogruaro Civic Tower’s Probabilistic Health Monitoring,” *J. Struct. Monit. Maint.*, 2(4):301-318.